Quantitative Analysis of Interdigitation Kinetics between a Polymer Melt and a Polymer Brush

ARTICLE · AUGUST 2013

DOI: 10.1021/ma4007335

Macromolecules

Article

pubs.acs.org/Macromolecules

Quantitative Analysis of Interdigitation Kinetics between a Polymer Melt and a Polymer Brush

Alexis Chennevière,[†] Eric Drockenmuller,[‡] Denis Damiron,[‡] Fabrice Cousin,[§] François Boué,[§] Frédéric Restagno,*[,†] and Liliane Léger*[,†]

[†]Laboratoire de physique des solides, CNRS, Université Paris-Sud, Bât. 510 Campus Universitaire, 91405 Orsay Cedex, France

[‡]Ingénierie des Matériaux Polymères, CNRS, Université Claude Bernard Lyon 1, 15 Boulevard Latarjet, 69622 Villeurbanne Cedex, France

[§]Laboratoire Léon Brillouin CEA, CNRS, CEA Saclay 91191, Gf sur Yvette Cedex, France

ABSTRACT: We present an investigation of the swelling dynamics of end-grafted hydrogenated polystyrene (h-PS) chains confined between a solid substrate and a deuterated polystyrene (d-PS) melt, based on neutron reflectometry experiments. The segment density profile of the grafted chains was measured for different annealing times. The kinetics of relaxation was quantified by measuring the amount of melt chains that have crossed the initial h-PS/d-PS sharp interface as a function of the annealing time. The dependence of this kinetics versus the molecular weight of the grafted chains, the melt chains, and the grafting density is investigated and compared to a proposed scaling model inspired from the previous work of Milner, McLeish, and O'Connor.[1,2] Moreover, the relaxation kinetics is found to highly depend on the polydispersity of the polymer brushes, and we propose a way for taking that parameter into account.

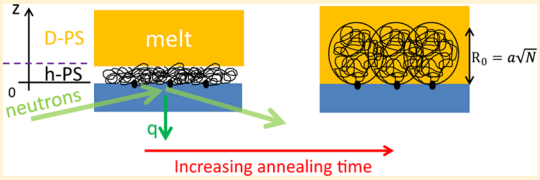

INTRODUCTION

End-tethered polymer chains have many interesting physical properties that gave rise to intensive theoretical and experimental studies in recent years. Those systems—called polymer brushes—can for example promote adhesion between a solid substrate and a compatible polymer network,[3,4] control the friction with a melt[5] or a network,[6−9] or modify the lubrication forces between the surfaces.[10] The conformation of the grafted chains and the way they entangle with the melt or the network determine the macroscopic properties of the interface and thus properties of composite materials.

De Gennes[11] studied the equilibrium conformation of a polymer brush immersed in a chemically identical polymer melt as a function of the different molecular parameters. The extension of the brush and the degree of penetration of the melt within the brush depend on the degree of polymerization of the grafted chains (N), the degree of polymerization of the melt chains (P), and the dimensionless grafting density $\sigma = (a/D)^2$, where D is the distance between two grafting points and a the size of one monomer (a = 6 Å for polystyrene[12]). When the degree of polymerization of the melt chains is larger than N, the extension of the brush and the degree of penetration no longer depend on P because the excluded volume interactions between the brush and the melt are screened. For σ lower than $\sigma_{max} = 1/\sqrt{N}$, the grafted chains adopt a Gaussian conformation with an extension equal to the radius of gyration $R_0 = a\sqrt{N}$ and the melt chains fully penetrate the brush. When σ is higher than σ_{max}, which corresponds to the so-called "dry brush" regime, the excluded volume interactions between the grafted chains can no longer be neglected. Therefore, the brush swells with an extension $L = aN\sigma$, and the melt chains do not fully penetrate the brush. The interpenetration between surface chains and bulk chains is responsible for entanglements which can give rise to the modification of the friction at the interface.[13−15] In particular, the role of these entanglements has been shown to play a key role in the enhancement of friction and low slip at the wall at low shear rates. In this paper, we will focus on the regime where $\sigma < \sigma_{max}$ since it is a regime of maximum stress transmission between the solid surface and the polymer melt and thus the regime where the chains at the surface can control adhesion and friction.

When the brush is not in contact with a melt, the grafted chains lie on the solid substrate forming a homogeneous layer of thickness z^* related to the grafting density by

$$\sigma = \frac{z^*}{Na} \tag{1}$$

For $\sigma < \sigma_{max}$, z^* is smaller than the radius of gyration of the grafted chains R_0 which implies that the end-tethered chains are confined inside this dry brush. When such a dry brush is put into contact with a compatible polymer melt below the glass transition temperature (T_g), the polymer brush stays in its confined state due to the lack of chains mobility. By heating the interface above T_g, interdigitation can take place, leading to a healing of the brush−melt interface. Previous neutron reflectivity experiments by Karim et al.[16] and molecular dynamic simulations by Pierce et al.[17] investigated the welding kinetics of polymer films in the melt state. They showed that

Received: April 9, 2013
Revised: July 9, 2013
Published: August 26, 2013

the early stages of interdiffusion are dominated by the motion of the chains ends and then follow the power laws predicted from reptation arguments. The situation of a brush−melt interface differs from the melt−melt interface because the broadening of the interface is limited to the equilibrium conformation of the grafted chains. The healing kinetics of such an interface has been first studied theoretically by O'Connor and McLeish[1] in the case of a brush in contact with a compatible network. They found that the kinetics can be divided into two steps. The first step corresponds to a fast penetration into the network of the free chain ends somewhat distant from the grafting point, thus leading to a metastable state called "strawberry runner".[1] In a second step, the end-tethered chains slowly reach their equilibrium conformation by a retraction mechanism along their original tube down to the grafting point. This mechanism is similar to the arm retraction of a star polymer, and its characteristic relaxation time depends exponentially on N.[18] Deutsch and Yoon[19] investigated this kinetics numerically with Monte Carlo methods for polymer chains tethered at one end or both ends. They found a two-stage process and were able to evidence the "strawberry runner" metastable state. Later, Geoghegan et al.[20] used neutron reflectivity to investigate this healing process between a polystyrene brush and a chemically identical cross-linked network. They measured the evolution of the density profile of the polymer brush as a function of the annealing time and studied the influence of the grafting density and the cross-link density of the network. They found a slowing down of the kinetics when the cross-link density or the grafting density were increased in accordance with the prediction of O'Connor and McLeish.[1] They also showed that the density profiles of the polymer brushes were different from those in a polymer melt. This has been explained by Vilmin et al.[21] by taking into account the elastic energy penalty of the network distortion during the interpenetration.

In the case of a polymer brush in contact with a melt, this elastic energy cost does not exist, and the interpenetration kinetics should differ from that observed by Geoghegan et al.[20] Moreover, because the melt chains can move by reptation, the entanglements between the grafted chains and the melt chains are not permanent. This can lead to constraint release process making the equilibration of the polymer brush quicker than when put into contact with a network. Clarke[22] characterized the interdigitation dynamics by neutron reflectivity for two identical polymer brushes in contact with two different melts. The corresponding density profiles were found in good agreement with self-consistent-field theory. The evolution of the density profile as a function of the annealing time was observed, but the exact dependency of the kinetics of relaxation on the different molecular parameters (N, P, and σ) was not determined. The brush−melt interdigitation kinetics is still an open question both from an experimental and a theoretical point of view.

In this paper, we present a quantitative determination of the interdigitation kinetics between a deuterated polystyrene melt (d-PS) and a hydrogenated polystyrene brush (h-PS) based on an extensive use of neutron reflectivity experiments. The measured relaxation times are compared to a scaling law inspired from the star polymer dynamics[2] and the model of O'Connor and McLeish.[1] Finally, the influence of the polymer brush polydispersity on this relaxation will be discussed.

EXPERIMENTAL SECTION

Synthesis of Amine End-Functionnalized Polystyrene. *Materials.* Amine-functionalized alkoxyamine (**1** in Figure 1) was

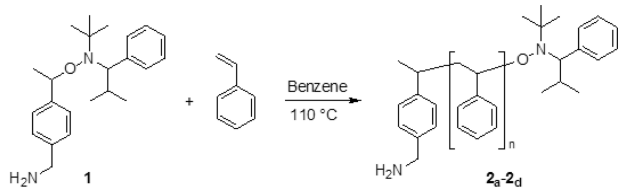

Figure 1. Synthesis of amine-functionalized polystyrene.

prepared as described previously,[23] and styrene (Acros, 99%) was distilled twice over calcium hydride. All other reagents and solvents were purchased from Aldrich and used as received.

General Procedure for the Synthesis of α-Aminopolystyrene Using NMRP. A solution of amine-functionalized alkoxyamine (85 mg, 0.24 mmol) in styrene (10 g, 96 mmol) and benzene (2 mL) was degassed by three freeze−pump−thaw cycles before being sealed under vacuum. After 15 h at 110 °C the polymerization medium was diluted in dichloromethane, precipitated twice in heptane, and dried, and α-aminopolystyrene (**2a** in Figure 1) was recovered as a white powder (Y = 50%, M_N = 110 000 g/mol, IP = 1.34). α-Aminopolystyrenes (**2b**) (M_N = 138 000 g/mol, IP = 1.32), (**2c**) (M_N = 204 000 g/mol, IP = 1.50), and (**2d**) (M_N = 250 000 g/mol, IP = 1.40) were obtained using the above procedure and by varying the initial ratio between **1** and styrene.

Grafted Layer Preparation and Characterization. Diethoxy(3-glycidyloxypropyl)methylsilane (97%, Sigma) was used to form a self-assembled reactive monolayer (SAM) on the native oxide layer of a silicon wafer[24,25] (2 in. Si(111) and 3 mm thick from Siltronix). The silicon wafers were cleaned in an ultrasonic bath and exposed to UV-ozone treatment so that silanol groups at the surface can react with the siloxane functionalities of the SAM precursors. Silicon wafers were put in a desiccator under vacuum. The system was then carefully heated so that vapor phase deposition of the silane takes place. After 8 h, the wafers were rinsed several times with anhydrous toluene and dried under vacuum. Ellipsometric measurements and AFM scans in tapping mode were carried out to check the thickness and the roughness of the SAM. SAM was found to be 1 nm thick which corresponds to the length of one siloxane molecule. Thus, molecules within the monolayer are oriented perpendicularly to the surface with epoxy groups at the air/SAM interface. On the top of this monolayer a thin layer of α-aminopolystyrene of number-average molecular weight M_N was spin-coated at 2000 rpm from a 3 wt % solution in toluene. The samples were then annealed in a vacuum oven at 140 °C to allow the NH_2 groups to chemically bond to the surface-tethered epoxy groups. The grafting density is efficiently controlled by the annealing time and increases with this annealing time. After several rinsing with toluene and drying under vacuum to remove the remaining solvent, the thickness z^* of the h-PS grafted layer was measured by ellipsometry. This thickness was found to be between 5 and 12 nm depending on the annealing time and M_N. Because the "grafting to" procedure is involved, z^* cannot be higher than the radius of gyration of the chains, which means that the dimensionless grafting density σ cannot be higher than σ_{max}. As a result, the polymer brushes are initially confined.

In order to characterize the interdigitation of the h-PS brush with a melt, a thin layer (∼400 nm) of d-PS of number-average molecular weight M_P (Polymer Source) was deposited upon of the brush. This layer was made by spin-coating a 5 wt % solution of d-PS in toluene onto a clean silicon wafer which was made hydrophilic thanks to UV-ozone treatment. The polymer film was then floated off in a bath of distilled water and transferred onto the polymer brush using a previously described technique.[22] The samples were then heated in a vacuum oven at temperatures T ranging from 120 to 150 °C during a time t_T. Samples were removed from the oven such that their temperature passed below T_g in a time of order of 1 mn, much shorter

dx.doi.org/10.1021/ma4007335 | Macromolecules 2013, 46, 6955−6962

than t_T. For each annealing time, neutron reflectivity measurements were carried out.

We used several annealing temperatures to cover a wide range of annealing times, by using the time−temperature superposition as expressed by the William, Landel, and Ferry equation[26] (WLF). According to the WLF equation, the relaxation time of a polymer at a certain temperature T, t_T, is related to the relaxation time at a chosen reference temperature t_{T_0} by $t_T/t_{T_0} = a_T$, where a_T is the "shift factor": for high molecular weight polystyrene (M_N > 100 kg/mol) and a reference temperature T_0 = 120 °C, the "shift factor" is given by[27]

$$\log(a_T) = \frac{-9.06(T - 120)}{69.8 + (T - 120)} \tag{2}$$

This allows to define for all samples an equivalent annealing time t calculated for a reference temperature of 120 °C by

$$t = a_T t_T \tag{3}$$

provided that T does not differ of more than 50 °C from the reference temperature.

At the end of each experimental session, the samples (reported in Table 1) were rinsed several times in toluene and carefully dried to

Table 1. Molecular Parameters of the Different Samples[a]

no.	M_N (kg/mol)	IP	$\sigma \times 10^{-3}$	M_P (kg/mol)	τ_{exp} (s)
1	110 (2a)	1.34	8.2	525	6.7×10^3
2	110 (2a)	1.34	15	525	1.3×10^4
3	110 (2a)	1.34	19	327	3.5×10^3
4	138 (2b)	1.32	14	327	1.4×10^4
5	138 (2b)	1.32	11	327	6.6×10^3
6	204 (2c)	1.50	9.0	525	8.0×10^4
7	204 (2c)	1.50	4.4	327	7.4×10^3
8	250 (2d)	1.40	7.5	525	1.1×10^6

[a]Molecular weight of the grafted chains M_N and their index of polydispersity IP, molecular weight of the melt chains M_P, the grafting density σ, measured by ellipsometry along with the fitted relaxation time τ_{exp} from eq 12.

verify by ellipsometry measurements that no chains had been neither detached from the substrates nor cleaved. The difference in thickness between the fresh brushes and the rinsed after use brushes has always been lower than 8 Å.

Neutron Reflectivity. Neutron reflectivity has been extensively used in the past and was found to be a powerful technique to characterize polymer brushes in a solvent[28,29] or a melt[22,30] and polymer−polymer interfaces.[16,31] Indeed, this technique gives information on the thickness and the profile of refractive index n for neutrons:

$$n(z) = 1 - \frac{\lambda^2}{2\pi}\rho(z) \tag{4}$$

where $\rho(z)$ is the scattering length density (SLD) of the material at distance z from the substrate. Since neutrons are scattered very differently by hydrogen and deuterium, deuteration of one chemical species provides enough contrast (quantified as the SLD difference) to characterize interfaces without changing the chemical interaction. In a binary blend composed of deuterated polystyrene (d-PS) melt and hydrogenated polystyrene brush (h-PS), the SLD is given by

$$\rho(z) = \phi(z)\rho_{h\text{-PS}} + (1 - \phi(z))\rho_{d\text{-PS}} \tag{5}$$

where $\phi(z)$ is the volume fraction of monomers belonging to the brush ($\rho_{d\text{-PS}} = 6.38 \times 10^{-6}$ Å^{-2} and $\rho_{h\text{-PS}} = 1.41 \times 10^{-6}$ Å^{-2}). Neutron reflectivity measurements were performed at the EROS time-of-flight reflectometer at Laboratoire Léon Brillouin, CEA, France. To access a broad wave vector range q (from 5.3×10^{-3} to 0.11 Å^{-1}), data were collected at two different angles (1.4° and 2.5°) with a neutron white beam covering wavelength from 2.5 to 29 Å. To get the corresponding density profiles $\phi(z)$ of the polymer brushes, we developed a fitting program that allows one to conserve the surface excess $z^* = \int_0^\infty \phi(z)\,dz$ between different annealing times. Since the polymer brush is not cleaved during the annealing, this condition is a crucial argument to state that the density profiles are physically relevant. This fitting program uses the optical matrix method[32] to compute the reflectivity and takes into account the angular resolution of the spectrometer. We used standard χ^2 minimization with a profile composed of a parabolic part continuously linked to an error function.

$$\phi(z) = \begin{cases} \phi_0\left(1 - \dfrac{z^2}{L^2}\right) & \text{for } z \le l \\ \phi_1\left(1 - \mathrm{erf}\left(\dfrac{z - b}{c}\right)\right) & \text{for } z > l \end{cases} \tag{6}$$

where ϕ_0, L, l, ϕ_1, b, and c are the parameters of the profile related by the condidition of continuity at $z = l$ and the condition on the surface excess ($\int_0^\infty \phi(z)\,dz = z^*$). Therefore, we are left with four fitting parameters. Such profiles have been previously used in the literature to fit polymer brush−polymer melt interfaces[33] and are in good agreement with self-consistent-field theory.[34] For all measured spectra, the normalized parameter χ^2 was lower than 1.5, which was our cutoff value to validate the quality of our fits.

RESULTS AND DISCUSSION

A typical example of reflectivity data is shown in Figure 2a,b for sample no. 6 after different annealing times. A gradual decrease in the reflectivity for wave vectors q ranging from 0.01 to 0.03 Å^{-1} is observed which shows that the interface between the melt and the grafted chains becomes smoother as the annealing time increases. After about 70 h ($t > 2.6 \times 10^5$ s) of annealing at 120 °C, the reflectivity curves become stationary and the system has reached its equilibrium state. Figure 2c shows the corresponding density profiles calculated by fitting the reflectivity data as explained above. The dashed line corresponds to the theoretical initial density profile without any interdigitation (assuming no roughness), the volume fraction ϕ being thus a step function where $\phi(z) = 1$ for $0 < z < z^*$. Increasing the annealing time, $\phi(z)$ decreases for $0 < z < z^*$ and increases for $z^* < z$, as a result from the penetration of the melt chains through the interface $z = z^*$ and of the unfolding of the grafted chains toward the melt. This evolution takes place until equilibrium is reached as schematically represented in Figure 3. Since $\sigma < \sigma_{max}$, the extension of the brush should be equal to the radius of gyration of the grafted chains[11] R_0. For the data shown in Figure 2, the radius of gyration is estimated to be $R_0 \simeq 300$ Å, which is in good agreement with the final extension of the brush measured experimentally. This is an additional argument to state that the system has reached equilibrium.

In order to provide a more quantitative analysis, two different quantities were measured as a function of the annealing time to quantify the equilibration time of the grafted chains. One possibility consists in computing the first moment of the density profile, $\Delta = 2(\int_0^\infty z\phi(z)\,dz)/z^*$, which represents the extension of the brush. However, this quantity is very sensitive to the fluctuations in the tail of the density profile. In that part of the density profile, the signal-to-noise ratio is the lowest inducing low experimental accuracy. An alternative consists in using an other quantity associated with the part of the density profile closer to the solid surface, which we will call the "degree of penetration" I:

dx.doi.org/10.1021/ma4007335 | Macromolecules 2013, 46, 6955−6962

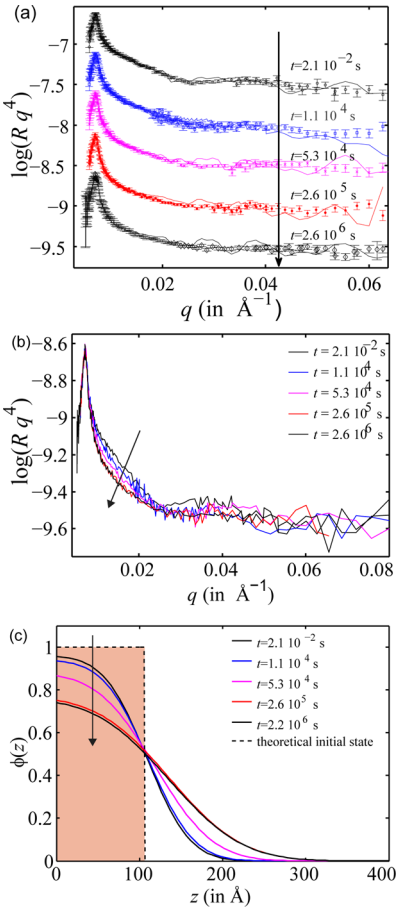

Figure 2. (a) Neutron reflectivity data for sample no. 6 for different annealing times. The curves are vertically shifted by 0.5 between two annealing times. Solid lines correspond to the fits. The arrow indicates the increasing time direction. (b) Neutron reflectivity for sample no. 6 unshifted and without error bars for a better visibility, showing explicitly the change with time of the spectra. (c) Corresponding density profiles. The colored area corresponds to the surface excess z^*.

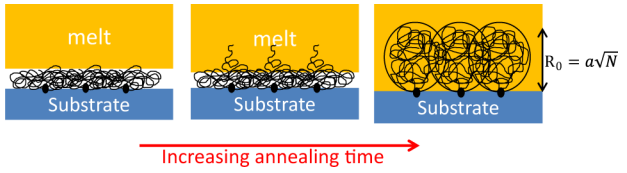

Figure 3. Scheme of the interdigitation process.

$$I = \frac{\int_0^{z^*} (1 - \phi(z))\, \mathrm{d}z}{z^*} \tag{7}$$

This quantity can be seen as the amount of melt chains that have crossed the interface $z = z^*$, replacing the part of the grafted chains which have extended into the melt. The evolution of I as a function of the annealing time t is plotted in Figures 4 and 5 for samples no. 6, 8 and no. 1, 2, 3, respectively. For all samples, a sharp increase in I is observed at the very beginning of the interdigitation and then the evolution of I slowly levels off toward its equilibrium value with a kinetics which depends on the molecular parameters of each samples. For all samples, the saturation of I corresponds to an extension of the brush comparable to the radius of gyration of the grafted

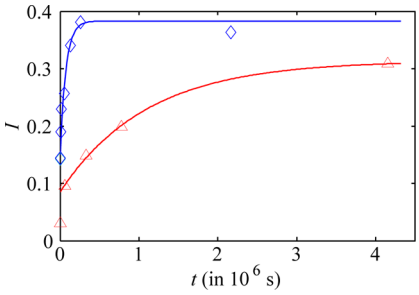

Figure 4. Evolution of the degree of penetration I as a function of the annealing time at 120 °C: (◇) sample no. 6: M_N = 204 kg/mol, M_P = 525 kg/mol, $\sigma = 9.0 \times 10^{-3}$; (△) sample no. 8: M_N = 250 kg/mol, M_P = 525 kg/mol, $\sigma = 7.5 \times 10^{-3}$. Solid lines represent the corresponding fits with $I = I_1 - I_0 e^{-t/\tau_{exp}}$.

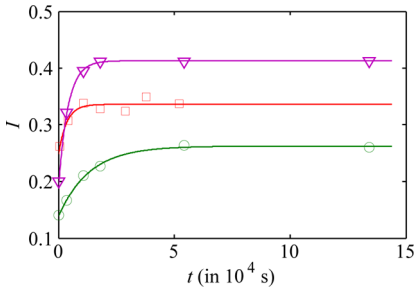

Figure 5. Evolution of the degree of penetration I as a function of the annealing time at 120 °C: (▽) sample no. 1: M_N = 110 kg/mol, M_P = 525 kg/mol, $\sigma = 8.2 \times 10^{-3}$; (○) sample no. 2: M_N = 110 kg/mol, M_P = 525 kg/mol, $\sigma = 15 \times 10^{-3}$; (□) sample no. 3: M_N = 110 kg/mol, M_P = 327 kg/mol, $\sigma = 19 \times 10^{-3}$. Solid lines represent the corresponding fits with $I = I_1 - I_0 e^{-t/\tau_{exp}}$.

chains which validates the use of the variable I to quantify the kinetics of interdigitation.

Regarding the measured equilibrium value of the "degree of penetration" I_{eq}, it can be noticed that I_{eq} depends on both M_N and σ. Such a dependency can indeed be inferred assuming a parabolic density profile with an extension equal to the radius of gyration R_0. Even though this analytic form is not the exact one, it is the simplest one close to the experimental density profile given that σ is not to close from σ_{max}. This parabolic density profile can be written as follows:

$$\phi(z) = \phi_0 \left(1 - \frac{z^2}{{R_0}^2}\right) \tag{8}$$

By developing the relation between ϕ and the thickness of the nonswollen brush z^*, one can express ϕ_0 as a function of N and σ:

$$\int_0^{\infty} \phi(z)\, \mathrm{d}z = z^* \Leftrightarrow \phi_0 = \frac{3}{2}\sigma\sqrt{N} \tag{9}$$

With this last expression, we can calculate I_{eq} as a function of the molecular parameters:

$$I_{eq} = \int_0^{z^*} \frac{1 - \phi(z)}{z^*}\, \mathrm{d}z = 1 - \frac{3}{2}\sigma\sqrt{N}\left(1 - \frac{\sigma^2 N}{3}\right) \tag{10}$$

According to this expression, I depends on both N and σ and can be written as a function of the unique variable σ/σ_{max}:

dx.doi.org/10.1021/ma4007335 | Macromolecules 2013, 46, 6955−6962

$$I_{eq} = 1 - \frac{3}{2}\frac{\sigma}{\sigma_{max}}\left(1 - \frac{1}{3}\left(\frac{\sigma}{\sigma_{max}}\right)^2\right) \quad (11)$$

The experimental values of I_{eq} as a function of σ/σ_{max} are plotted in Figure 6 and compared with the predictions of eq 11.

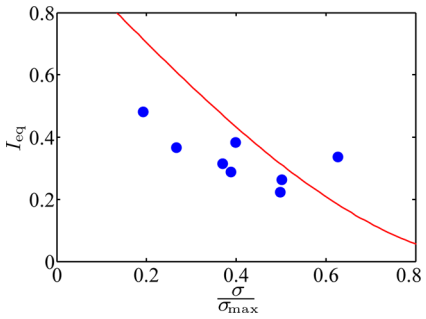

Figure 6. Evolution of I_{eq} as a function of σ/σ_{max}. The solid line corresponds to the prediction of eq 11.

The experimental points show a tendency similar to the prediction of eq 11 and present a qualitative agreement even if they do not follow exactly the predictions. The difference between the model and the experimental data can be due to the assumption of a parabolic profile, which does not correspond exactly to the measured profiles. Computing the density profiles using self-consistent field theory could be a useful tool to reduce that discrepancy and better predict the evolution of I_{eq} as a function of σ/σ_{max}.

Concerning the kinetics of relaxation, all data can be fitted by an exponential law:

$$I = I_1 - I_0 e^{-t/\tau_{exp}} \quad (12)$$

where τ_{exp}, I_0, and I_1 are the fitting parameters. It is worth noting that even if before interdigitation I should be equal to 0, this assumption is only valid for an initial interface without any roughness. That is why we chose $I_1 \neq I_0$. In order to probe that initial roughness, the experimental density profile of a unannealed polymer brush in contact with a melt was measured, as shown in Figure 7 for sample no. 8. When the

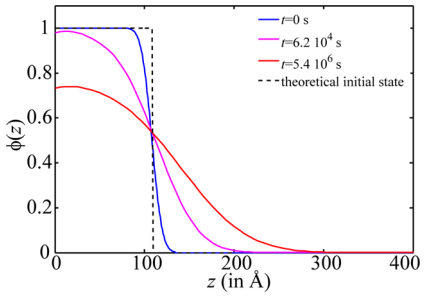

Figure 7. Density profiles for sample no. 8 after different annealing times.

sample has not been annealed above T_g, the density profile is only composed of an error function which width c = 13 Å. As the sample is annealed above T_g, the parabolic part of the profile appears and the interdigitation process takes place until the extension of the brush reaches the radius of gyration of the grafted chains with the characteristic relaxation time τ_{exp}. Experimentally, this kinetics of equilibration appears to be an increasing function of the molecular weight of the grafted chains, the grafting density, and the molecular weight of the melt chains. It can be noticed in Figure 4 that τ_{exp} (reported in Table 1) is very sensitive to the molecular weight of the grafted chains. An increase of M_N from 204 to 250 kg/mol leads to an increase of τ_{exp} form 8.0×10^4 to 1.1×10^6 s. This clearly demonstrates that the dynamics of end tethered chains strongly differs from reptation.

Model. Indeed, end-tethered chains cannot move by a reptation process as linear chains do. They can only equilibrate by arm retraction such as star polymers, which has been extensively studied theoretically and experimentally.[2,18] Milner and McLeish[2] computed the arm retraction time of a star polymer in a melt of identical star polymers. They found that the characteristic time for an arm to retract τ_{arm} is given by

$$\tau_{arm} \sim \frac{a^2 N_e}{D_{eff}}\left(\frac{N}{N_e}\right)^{(1/2)+[\alpha/(\alpha+1)]} \exp\left(\frac{15}{4(\alpha+1)(\alpha+2)}\frac{N}{N_e}\right) \quad (13)$$

where N_e is the number of monomers between two entanglements and D_{eff} is the effective diffusion coefficient of the free end of the grafted chains. α is the dynamic dilution exponent[35] which takes into account the fact that entanglements along the grafted chains are not equivalent. Since entanglements close to the grafted point relax much slower than the ones at the free end, the latter can be thought as completely mobile. Thus, the grafted chains see a diluted entanglement network of ideal chains which can be viewed as a semidilute solution under Θ conditions. For star polymer melts, D_{eff} is twice the Rouse diffusion coefficient. In our experimental system, the free ends penetrate the melt thanks to a constraint release process which corresponds to the renewal of the tube of the end tethered chains controlled by the reptation of the melt chains $\tau_{rep}(P)$, where P is the degree of polymerization of the melt chains. According to ref 36 the constraint release diffusion coefficient D_{CR} is given by $D_{CR} = D_0 N^{-1} P^{-3}$. Assuming that $D_{eff} = D_{CR}$ and taking[35] $\alpha = 4/3$, τ_{arm} becomes

$$\tau_{arm} = \tau_0 N^{2.07} P^3 \exp\left(0.48\frac{N}{N_e}\right) \quad (14)$$

where τ_0 is a characteristic molecular time which depends on N_e and on the monomer/monomer friction coefficient. The scaling of eq 14 does not predicts the effect of the grafting density observed experimentally. Indeed, the grafting density plays a role in terms of energy of confinement for the grafted chains in the dry layer; the lower σ, the higher the confining energy. The initial energy of confinement F_{conf}^{ini} is given by a simple scaling:[37]

$$\frac{F_{conf}^{ini}}{kT} = \beta\frac{R_0^2}{z^{*2}} = \frac{\beta}{\sigma^2 N} \quad (15)$$

where β is a prefactor. At equilibrium, the chains are no longer confined, which gives $F_{conf}^{eq}/kT = \beta$. The relaxation of a grafted chain can be viewed as driven by the energy gap of confinement with a characteristic relaxation time τ_{arm}. This would mean that the relaxation time τ_{rel} of the system follows the Arrhenius law $\tau_{rel} \propto \tau_{arm} \exp[(F_{conf}^{eq} - F_{conf}^{ini})/kT]$ leading to the following expression for τ_{rel}:

$$\tau_{rel} = \tau_0 N^{2.07} P^3 \exp\left(0.48\frac{N}{N_e}\right)\exp\left(-\frac{\beta}{\sigma^2 N}\right) \quad (16)$$

dx.doi.org/10.1021/ma4007335 | Macromolecules 2013, 46, 6955−6962

which is an increasing function of the grafting density, as observed experimentally (Figure 5 and Table 1).

The experimental relaxation time τ_{exp} is plotted in Figure 8 as a function of the theoretical dimensionless relaxation time

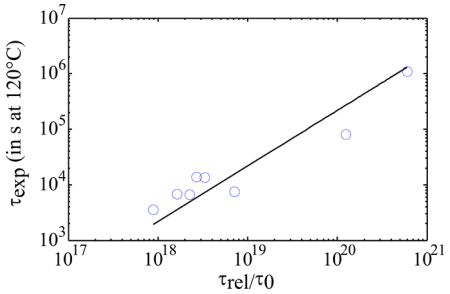

Figure 8. Plot of the experimental relaxation time as a function of τ_{rel}/τ_0 (eq 16) for $\beta = 0.15$.

τ_{rel}/τ_0 where β is fitted so that the experimental points are the closest from a straight line of slope 1. The optimum value for β was found to be $\beta = 0.15$, leading to $\tau_0 = 2.2 \times 10^{-15}$ s. Concerning the value of τ_0, an expectation can be deduced from an independent measurement of the diffusion coefficient D_0 for polystyrene[36] ($D_0 = 2.6 \times 10^{-5}$ m^2 s^{-1}), leading to $\tau_0 = 3.2 \times 10^{-15}$ s. The order of magnitude of τ_0 resulting from the fit is found in quite good agreement with the expected value. As regard to the parameter β, there is no estimated value available in the literature to our knowledge.

It can be observed in Figure 8 that the scaling predicted by eq 16 appears to be in good agreement with the experimental data except for two points corresponding to samples no. 6 and 7 that present a faster dynamics. Among the possible explanations, this difference might be due to the relatively higher polydispersity of those samples. Indeed, τ_{rel} is dramatically sensitive to N because of the exponential dependency; thus, a small difference in the molar mass distribution of the samples will broaden the spectrum of relaxation time and change the overall dynamics of the system. Moreover, the dependency on σ does not take into account the entanglements distribution between the grafted chains. For lower σ, there are more available entanglements between the melt chains and the grafted chains susceptible to relax by constraint release. When σ increases, the brush−melt entanglements are replaced by brush−brush entanglements relaxing with a different kinetics leading to a complex collective behavior. Such a difference between the two kinds of entanglements is not taken into account in the present model. Anyhow, this model seems to capture the main dependencies on the different molecular parameters of the system. It represents a step toward a full description of the collective behavior of polymer brushes, which remains a open question and calls for additional theoretical studies.

Effect of Polydispersity. In order to see whether the polydispersity could be responsible for the change in dynamics, an effective relaxation time τ_{eff} for polymer brushes with different degree of polymerization distributions $n(N)$ at different grafting densities was calculated. By assuming that the grafted chains are independent of each other, τ_{eff} is given by

$$\frac{1}{\tau_{eff}} = \int \frac{n(N)}{\tau_{rel}(N)}\,dN \tag{17}$$

Among the several expressions of $n(N)$ available in the literature,[38] we chose the so-called log-normal distribution given by

$$n(N) = \frac{1}{\sqrt{2\pi}}\frac{1}{N\Delta}\exp\left(-\frac{(\log(N) - \log(N_0))^2}{2\Delta^2}\right) \tag{18}$$

$$N_0 = N_w \exp\left(-\frac{3}{2}\Delta^2\right)$$

$$\Delta^2 = \log\left(\frac{N_w}{N_n}\right) = \log(IP) \tag{19}$$

where N_n and N_w are respectively the number-average and weight-average degree of polymerization and IP the polydispersity index.

Because there is no analytic form for τ_{eff}, we computed numerically τ_{eff} as a function of N_n for different IP and plotted the results in Figure 9. τ_{eff} decreases dramatically when the

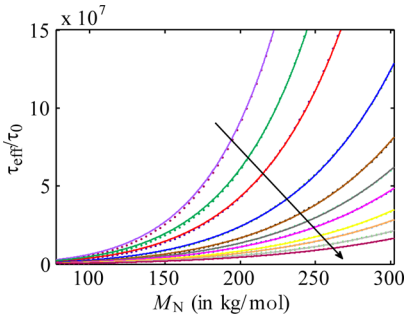

Figure 9. Effective relaxation time as a function of the molar mass M_n of the grafted chains for indexes of polydispersity ranging from 1.1 to 1.61 and an initial thickness $z^* = 100$ Å. The arrow indicates increasing polydispersity indices IP. From the upper to the lower curve IP = [1.11; 1.15; 1.19; 1.26; 1.32; 1.36; 1.40; 1.44; 1.50; 1.55; 1.61].

polydispersity increases. This is in qualitative agreement with our experimental data. Indeed, when the polydispersity increases at fixed N_n, the degree of polymerization distribution is enriched in small chains which have a strong contribution in τ_{eff}.

τ_{eff} was fitted using the following arbitrary function

$$f(N_n) = aN_n^{2.07}\exp(bN_n) \tag{20}$$

and the evolution of the fitting parameters a and b as a function of IP are plotted in Figure 10. Both a and b decrease with the increase in IP and seem to follow a power law $a \propto IP^{-4}$ and $b \propto IP^{-2.8}$. By inserting those two power laws in the expression of τ_{rel}, the effective relaxation time of the system can be written as

$$\tau_{eff} = \tau_0 IP^{-4} N^{2.07} P^3 \exp\left(\frac{1}{IP^{2.8}}\left(\frac{N}{N_e} - \frac{0.15}{\sigma^2 N}\right)\right) \tag{21}$$

The experimental relaxation time τ_{exp} was then plotted as a function of τ_{eff}/τ_0 in Figure 11 where it can be observed that the agreement between the experimental data and the model is better than without taking into account the polydispersity. In particular, the two points corresponding to samples no. 6 and 7 with the highest polydispersity (IP = 1.5) are now well aligned with the others. Other families of fitting function such as $g(N_n) = aN_n^c \exp(bN_n)$ have been used to fit the simulated values of τ_{eff}. The fits were not better, and the presence of an additional

dx.doi.org/10.1021/ma4007335 | Macromolecules 2013, 46, 6955−6962

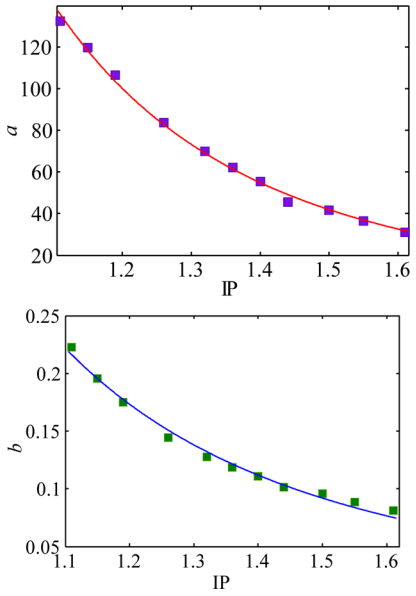

Figure 10. Evolution of the fitting parameters a and b as a function of the index of polydispersity (IP) and corresponding fit with a power law.

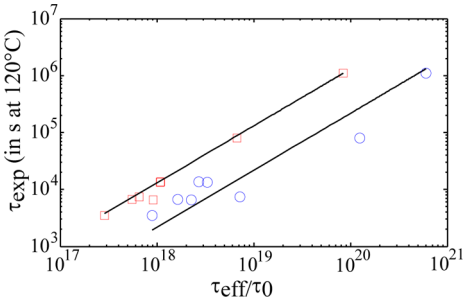

Figure 11. A log−log plot of the experimental relaxation time τ_{exp} as a function of (□) τ_{eff}/τ_0 and (○) τ_{rel}/τ_0. The solid lines corresponds to $\tau_{exp} \propto \tau_{eff}$.

fitting parameter makes the analysis more complex and does not reveal simple dependency on the IP.

We emphasize that we found numerically that the influence of the shape of the molar mass distribution has a real importance on the effective time of relaxation and that the values of N_n and IP are not sufficient to predict the dynamics. Therefore, the proposed phenomenological scaling for polydisperse polymer brushes should remain valid only for a log-normal molar mass distribution and cannot be considered as a general law. The polydispersity is clearly a crucial parameter for the relaxation of polymer brushes or star polymers, and the two first moments of the polymer chain length distribution are not sufficient to fully characterize the dynamics of polydisperse tethered chains.

CONCLUSION

We manage to get physically relevant segment density profiles for series of hydrogenated polystyrene brushes immersed in a deuterated polystyrene matrix as a function of the annealing time. Neutron reflectivity experiments show the relaxation of the grafted chains until they reach equilibrium which kinetics were quantified by measuring the "degree of penetration" between the melt and the brush. Indeed, this "degree of penetration" is accurately determined by neutron reflectivity measurements and allows to precisely analyze the effect of the molecular parameters of the system on the relaxation kinetics. We have shown that this relaxation kinetics is mainly fixed by the polymerization index of the grafted chains (exponential dependency) and more weakly affected by the polymerization index of the melt chains and by the grafting density. These dependencies were found to well agree with a scaling prediction inspired from the star polymer melt theory.

We also found that the polydispersity of the polymer brushes has a huge impact on the kinetics of relaxation. This was expected, but more quantification of this effect is very important from the applied point of view of friction and adhesion at polymer interfaces. A phenomenological scaling law valid for a log-normal distribution of polymer weights was proposed to take the polydispersity into account. Our next step will indeed be the evolution of this dynamics for stretched chains in friction or adhesion experiment.

AUTHOR INFORMATION

Corresponding Author

*E-mail: frederic.restagno@u-psud.fr (F.R.); liliane.leger@u-psud.fr (L.L.).

Notes

The authors declare no competing financial interest.

ACKNOWLEDGMENTS

E.D. gratefully acknowledge the financial support from the Institut Uninversitaire de France (IUF). We benefited from an ANR grant (WAFPI project).

REFERENCES

(1) O'Connor, K.; McLeish, T. *Macromolecules* **1993**, *26*, 7322−7325.
(2) Milner, S. T.; McLeish, T. C. B. *Macromolecules* **1997**, *30*, 2159−2166.
(3) Raphael, E.; De Gennes, P. G. *J. Phys. Chem.* **1992**, *96*, 4002−4007.
(4) Brochard-Wyart, F.; De Gennes, P. G.; Leger, L.; Marciano, Y.; Raphael, E. *J. Phys. Chem.* **1994**, *98*, 9405−9410.
(5) Sides, S. W.; Grest, G. S.; Stevens, M. J.; Plimpton, S. J. *J. Polym. Sci., Part B: Polym. Phys.* **2003**, *42*, 199−208.
(6) Léger, L.; Hervet, H.; Bureau, L. *C. R. Chim.* **2006**, *9*, 80−89.
(7) Casoli, A.; Brendlé, M.; Schultz, J.; Auroy, P.; Reiter, G. *Langmuir* **2001**, *17*, 388−398.
(8) Vilmin, T.; Raphaël, E. *J. Adhes.* **2006**, *82*, 517−526.
(9) Cohen, C.; Restagno, F.; Poulard, C.; Léger, L. *Soft Matter* **2011**, *7*, 8535−8541.
(10) Klein, J.; Kamiyama, Y.; Yoshizawa, H.; Israelachvili, J. N.; Fredrickson, G. H.; Pincus, P.; Fetters, L. J. *Macromolecules* **1993**, *26*, 5552−5560.
(11) De Gennes, P. G. *Macromolecules* **1980**, *13*, 1069−1075.
(12) Cotton, J. P.; Decker, D.; Benoit, H.; Farnoux, B.; Higgins, J.; Jannink, G.; Ober, R.; Picot, C.; Des Cloizeaux, J. *Macromolecules* **1974**, *7*, 863−872.
(13) Léger, L.; Raphaël, E.; Hervet, H. *Polymers in Confined Environments*; Springer: Berlin, 1999; pp 185−225.
(14) Durliat, E.; Hervet, H.; Leger, L. *Europhys. Lett. (EPL)* **1997**, *38*, 383−388.
(15) Pastorino, C.; Binder, K.; Müller, M. *Macromolecules* **2009**, *42*, 401−410.
(16) Karim, A.; Mansour, A.; Felcher, G. P.; Russell, T. P. *Phys. Rev. B* **1990**, *42*, 6846.
(17) Pierce, F.; Perahia, D.; Grest, G. S. *Europhys. Lett. (EPL)* **2011**, *95*, 46001.
(18) De Gennes, P. *J. Phys. (Paris)* **1975**, *36*, 1199−1203.
(19) Deutsch, J.; Yoon, H. *Macromolecules* **1994**, *27*, 5720−5728.

(20) Geoghegan, M.; Clarke, C. J.; Boué, F.; Menelle, A.; Russ, T.; Bucknall, D. G. *Macromolecules* **1999**, *32*, 5106−5114.
(21) Vilmin, T.; Tardivat, C.; Léger, L.; Brown, H.; Raphael, E. *Europhys. Lett. (EPL)* **2004**, *68*, 543−549.
(22) Clarke, C. *Polymer* **1996**, *37*, 4747−4752.
(23) Dao, J.; Benoit, D.; Hawker, C. J. *J. Polym. Sci., Part A: Polym. Chem.* **1998**, *36*, 2161−2167.
(24) Dorvel, B.; Reddy, B.; Block, I.; Mathias, P.; Clare, S. E.; Cunningham, B.; Bergstrom, D. E.; Bashir, R. *Adv. Funct. Mater.* **2010**, *20*, 87−95.
(25) Luzinov, I.; Julthongpiput, D.; Liebmann-Vinson, A.; Cregger, T.; Foster, M.; Tsukruk, V. *Langmuir* **2000**, *16*, 504−516.
(26) Flory, P. J. *Principles of Polymer Chemistry*; Cornell University Press: Ithaca, NY, 1953.
(27) Tassin, J. F.; Monnerie, L.; Fetters, L. J. *Macromolecules* **1988**, *21*, 2404−2412.
(28) Marzolin, C.; Auroy, P.; Deruelle, M.; Folkers, J. P.; Léger, L.; Menelle, A. *Macromolecules* **2001**, *34*, 8694−8700.
(29) Elliott, I. G.; Mulder, D. E.; Träskelin, P. T.; Ell, J. R.; Patten, T. E.; Kuhl, T. L.; Faller, R. *Soft Matter* **2009**, *5*, 4612.
(30) Clarke, C.; Jones, R.; Edwards, J.; Shull, K.; Penfold, J. *Macromolecules* **1995**, *28*, 2042−2049.
(31) Russell, T. *Physica B* **1996**, *221*, 267−283.
(32) Penfold, J.; Thomas, R. K. *J. Phys.: Condens. Matter* **1990**, *2*, 1369.
(33) Jones, R.; Norton, L.; Shull, K.; Kramer, E.; Felcher, G.; Karim, A.; Fetters, L. *Macromolecules* **1992**, *25*, 2359−2368.
(34) Shull, K. R. *J. Chem. Phys.* **1991**, *94*, 5723.
(35) Colby, R. H.; Rubinstein, M. *Macromolecules* **1990**, *23*, 2753−2757.
(36) Green, P. F.; Mills, P. J.; Palmstrøm, C. J.; Mayer, J. W.; Kramer, E. J. *Phys. Rev. Lett.* **1984**, *53*, 2145−2148.
(37) de Gennes, P. G. *Scaling Concepts in Polymer Physics*; Cornell University Press: Ithaca, NY, 1979.
(38) Devos, W.; Leermakers, F. *Polymer* **2009**, *50*, 305−316.